Thin Solid Films 519 (2011) 4220–4224

Contents lists available at ScienceDirect

Thin Solid Films

journal homepage: www.elsevier.com/locate/tsf

Investigation of the effects of bottom anti-reflective coating on nanoscale patterns by laser interference lithography

Eun-Mi Park [a], Jinnil Choi [a], Byung Hyun Kang [a], Ki-Young Dong [a], YunKwon Park [b], In Sang Song [b], Byeong-Kwon Ju [a,*]

[a] Display and Nanosystem Laboratory, College of Engineering, Korea University, Republic of Korea
[b] Future IT Center Communication Laboratory, Samsung Advanced Institute of Technology, Republic of Korea

ARTICLE INFO

Article history:
Received 18 May 2010
Received in revised form 16 February 2011
Accepted 16 February 2011
Available online 24 February 2011

Keywords:
Bottom anti-reflective coating
Laser interference lithography
Nanoscale patterning

ABSTRACT

Enhanced resolution of the structures can be achieved by employing the bottom anti-reflective coating (BARC) material in laser interference lithography process. The purpose of the BARC is to control the reflection of light at the surface of the wafer to minimize the effects caused by reflection. Lloyd's mirror interferometer is utilized for the experiment with 257 nm wavelength Ar-Ion laser used as the light source to generate one-dimensional nanoscale patterns. By adjusting reflectivity through application of the BARC material, scattering of the patterns are reduced. The effects of BARC material are explored to confirm the reduction of the vertical standing wave, which is the main cause of undesirable nanoscale patterns. It is also highlighted that improvements through utilization of BARC material enables smaller pattern size with a set pitch size by controlling the exposure energy.

1. Introduction

In recent years, there is soaring demand for technology to create components of nano- scale integrated circuits in the field, such as biotechnology and nanotechnology display, IT industry, environment, and energy. The technologies utilized to fabricate nano-structures include nano-imprint lithography, e-beam lithography, scanning probe-based writing, and focused ion-beam etching. However, most of these technologies require high equipment prices and face challenges in producing large patterns spanning several nano-meters [1,2]. In contrast, laser interference lithography (LIL) is considered to be highly efficient, in terms of its maskless and quick process, and its capability of generating patterns over a large area. LIL is a well established concept where an interference pattern between two coherent light waves are set up and recorded over a photosensitive layer to produce periodic structures. Moreover, LIL has been applied to fabricate one, two and multi-dimensional patterns through structural modification of the apparatus and utilization of multiple beams [1–5]. However, the vertical standing waves caused by the reflection from the Si substrate results in generating undesired patterns [6]. To prevent these problems, anti-reflective coating is widely used where it controls the reflection of the laser light source at the surface of the wafer [7–9].

The main focus of this study is on the investigation of the effects of bottom anti-reflective coating (BARC) material in LIL for generating more uniform nanoscale structures with the usage of a robust positive photoresist and BARC. The effects are further explored through the reduction in the size of the patterns by controlling the angle between two beams and the energy applied.

2. Experimental details

The experiment employed a Lloyd's mirror interferometer with Ar-Ion ($\lambda = 257$ nm) laser as shown in Fig. 1(a). The laser with 515 nm wavelength was frequency doubled by a beta-barium borate crystal [10]. The laser beam goes through the spatial filter which was then expanded 27 times. Pinhole was applied for noise reduction and iris for the exposure beam area selection. As shown in Fig. 1(b), a single exposure results in one-dimensional line patterns and 90° rotation of the sample between double exposures produces two-dimensional dot patterns.

In order to investigate the effects of BARC, case studies with and without the application of BARC, commercialized anti-reflective resin (DUV-30J, Brewer Science), were performed. Additionally, the variation of LIL angle (θ, half angle between the two incident beams) and the applied energy dose to the sample were explored. Firstly, a 3 cm × 3 cm Si substrate was cleaned with acetone, methanol, and deionized water. For the experiments without the usage of BARC, hexamethyldisilazane (HMDS) was spin coated for 30 s at 2000 rpm on the bare silicon substrate to improve adhesion between the Si substrate and the photoresist (DHK-BF424, DongJin). The photoresist, chosen for 257 nm wavelength laser, was then spin coated for 25 s at

* Corresponding author. Tel.: +82 2 3290 3237; fax: +82 2 3290 3791.
E-mail address: bkju@korea.ac.kr (B.-K. Ju).

0040-6090/$ – see front matter © 2011 Elsevier B.V. All rights reserved.
doi:10.1016/j.tsf.2011.02.054

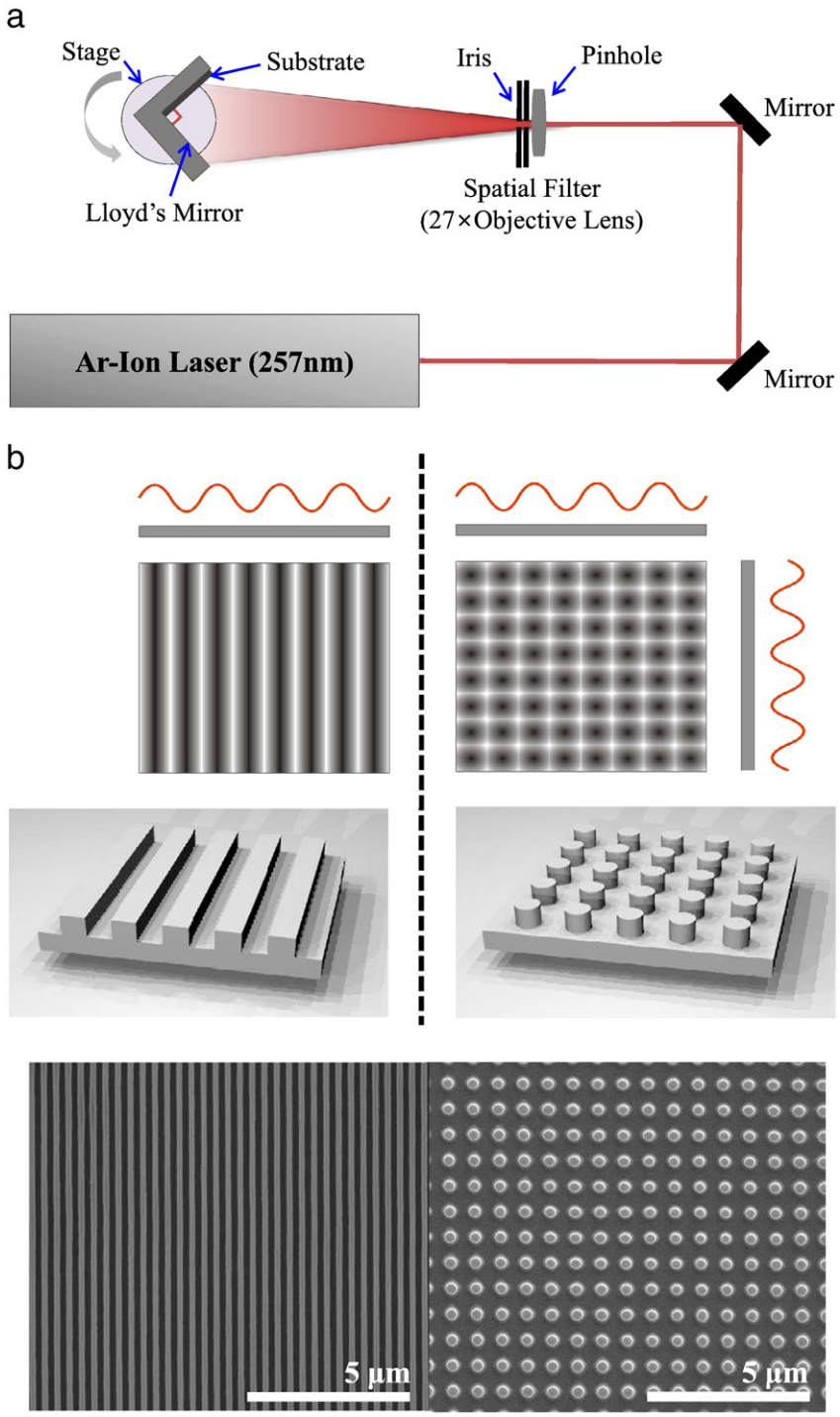

Fig. 1. (a) Overview of the LIL apparatus; and (b) SEM images of (left) one-dimensional and (right) two-dimensional patterns.

3000 rpm, and baked at 110 °C for 60 s. On the other hand, for the experiments with the usage of BARC, BARC materials were spin coated for 25 s at 3000 rpm on Si substrates resulting in around 492 nm thickness, measured by a surface profiler. The photoresist was then spin coated on top of BARC for 25 s at 3000 rpm without using HMDS, with the resulting thickness of around 472 nm, which was then baked at 110 °C for 60 s. Once the exposure energy was set at the desired dose using the optical power/energy meter, the sample was exposed by the laser. Next, following the post exposure baking at 110 °C for 60 s, the sample was developed according to time conditions. Finally, scanning electron microscopy (SEM, Hitachi S4800, 10 kV) images were taken for each sample. The series of case studies were identically prepared in this manner in order to observe the effects of BARC and especially to investigate the reduction in the size of the patterns by controlling LIL angle and the energy dose applied.

3. Results and discussion

Fig. 2 shows the comparison between samples with and without the application of BARC for one and two-dimensional patterns. The exposure dose was set to be 12 mJ/cm^2, identical experimental procedures were performed for each case. For the samples with the

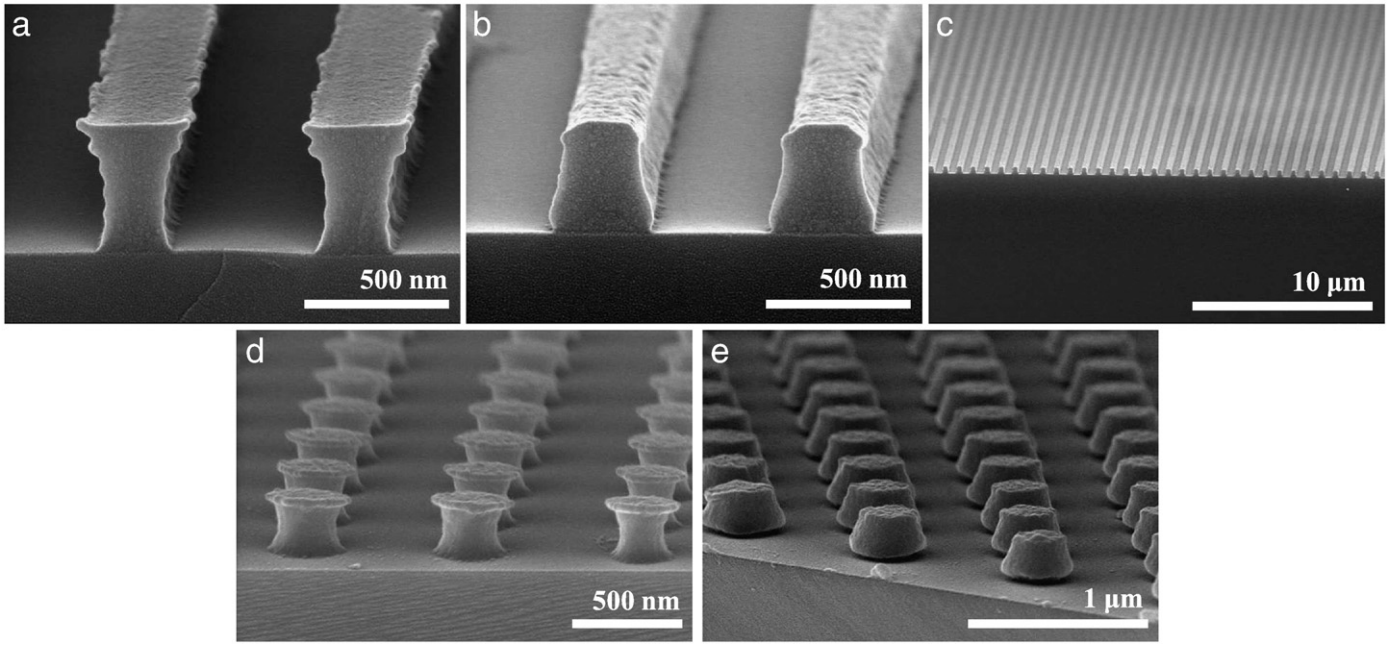

Fig. 2. SEM images of one-dimensional patterns (a) without BARC; (b) and (c) with BARC. Two-dimensional patterns (d) without BARC and (e) with BARC.

photoresist only, shown in Fig. 2(a) and (d), inconsistent shapes could be observed. As the vertical standing waves were caused from the reflection from the Si substrate, the width of the pillar was reduced as it is closer to the substrate and irregular wall surface could also be observed. These agree with the findings from previously reported work [7–11]. By applying the BARC materials, improvements on the patterns could be clearly seen in Fig. 2(b) and (e). With the introduction of the BARC materials, the patterns show more uniformity and stability, inconsistent shapes and irregular wall surfaces reduced, preventing the possibilities of the collapse of the structures. Additionally, pattern footing and T-top phenomena from the development process were significantly reduced. Since the enhancements of the patterns were confirmed, the possibility to fabricate smaller pattern sizes was investigated, highlighting the effects of the BARC materials. Conventional method of reducing the pitch and pattern size involves applying different LIL angles according to Eq. (1).

The relationship between the pitch of the pattern (Λ) and the angle between the two incident beams (2θ) can be expressed as follows:

$$\Lambda = \frac{\lambda}{2\sin\theta}. \quad (1)$$

By observing Fig. 3, it is clear that the changes in pitch and pattern size follow the theoretical values calculated from the equation. The comparison of sizes is itemized below in Table 1. The difference

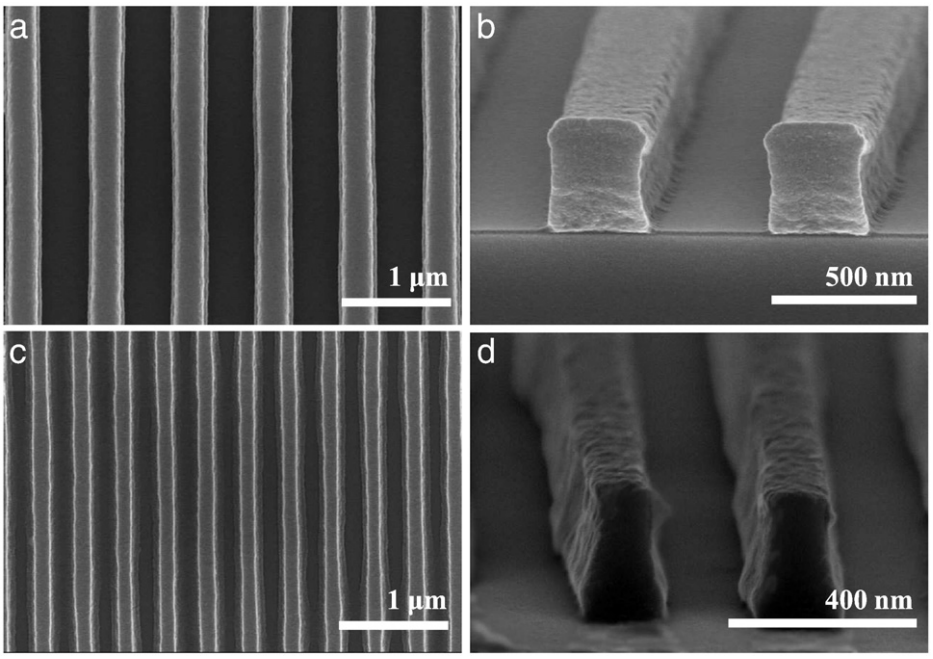

Fig. 3. SEM images of one-dimensional patterns at different angles of (a) & (b) 10 and (c) & (d) 20°.

Table 1
Comparison between theoretical and actual pitch sizes of the fabricated patterns.

LIL Angle	Theoretical Pitch Size	Measured Pitch Size	Measured Pattern Size
10°	740 nm	~742 nm	~350 nm
20°	376 nm	~380 nm	~160 nm

between measured and calculated pitch sizes was minimal which confirms the validity of Eq. (1). In addition, it could be observed that the fabricated pattern size was approximately half of the measured pitch size. However, as shown in Fig. 3(c) and (d), increasing the LIL angle leads to less uniform patterns due to the size limitations of LIL process.

To further investigate the effect of the BARC materials, the applied energy dose was varied instead of the LIL angle. By increasing the energy dose, although the pitch size was set to be around 770 nm, the pattern size was decreased down to 190 nm. Fig. 4 shows the top and cross sectional views of the line patterns at four different energy doses applied. The energy doses were 9, 12, 13.5, and 18 mJ/cm^2, resulting in pattern sizes of 390, 340, 290 and 190 nm, itemized in Table 2. It is apparent that increasing the applied dose results in smaller pattern size, less than the quarter of the pitch size observed from this experiment. The inverse linear relationship between energy dose and pattern size was also confirmed. Although the smallest pattern size was found to be 190 nm, which is larger than that from increasing LIL angle to 20° (around 160 nm), the uniformity of the patterns were significantly improved, as shown in Fig. 4(e)–(h). This again highlights the effect of the BARC materials where up to 190 nm pattern size, improved uniformity and stability were achieved over an area of 3×3 cm^2.

4. Conclusions

The effects of the BARC materials were studied for generating nanoscale patterns by LIL. Significant reduction of the vertical standing waves were observed, which resulted in enhancements of the pattern size reduction. Investigations on decreasing the pattern size were also performed, with the smallest line pattern size of

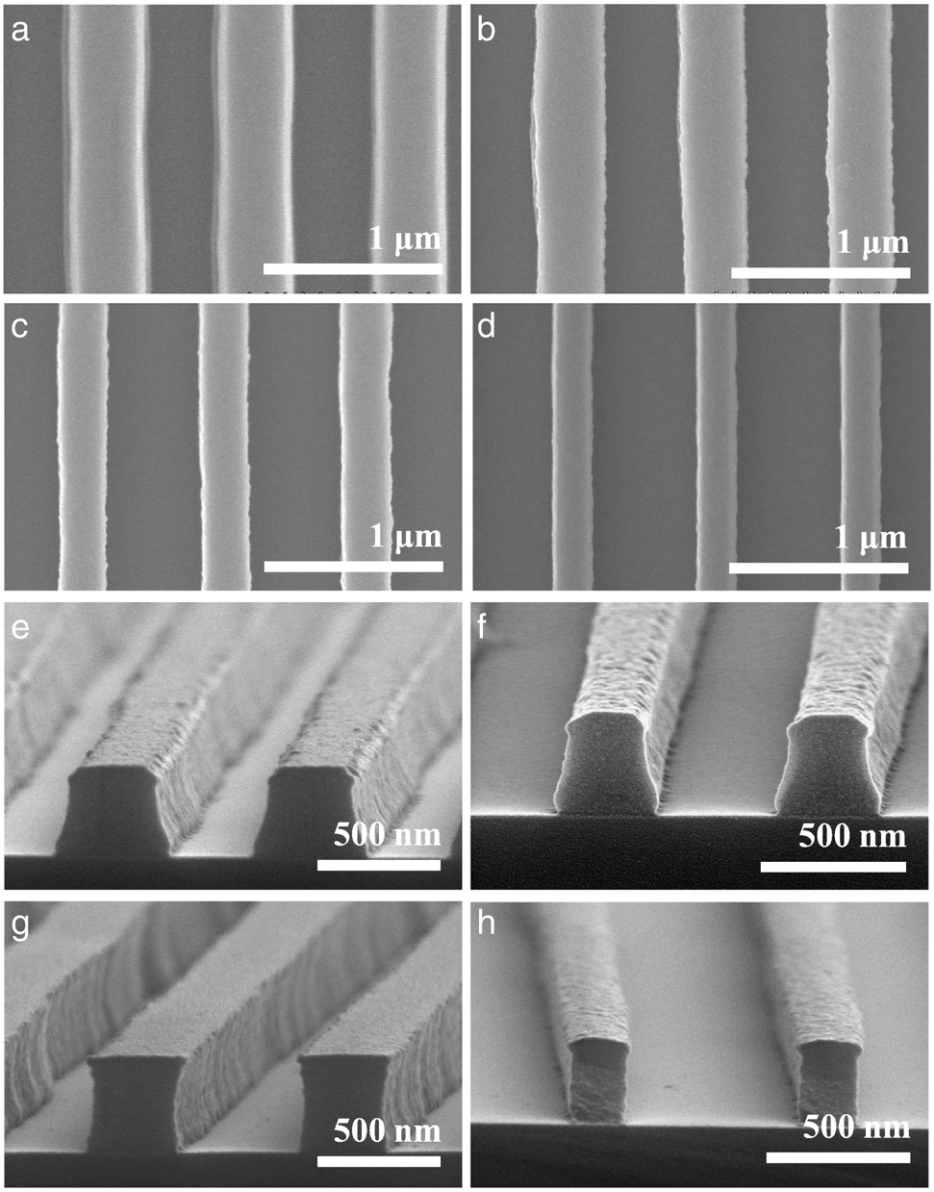

Fig. 4. SEM images of patterns at different exposure energy doses (a) & (e) 9, (b) & (f) 12, (c) & (g) 13.5, and (d) & (h) 18 mJ/cm^2 with pattern sizes of 390, 340, 290, and 190 nm respectively.

Table 2
Pitch and pattern sizes at different energy doses applied.

Energy dose (mJ/cm^2)	Pitch Size (nm)	Pattern Size (nm)	Size Ratio (Pitch:Pattern)
9	~770	390	1.97 : 1
12		340	2.27 : 1
13.5		290	2.66 : 1
18		190	4.05 : 1

190 nm over an area of $3 \times 3\ cm^2$ to be achieved, while maintaining the uniformity and improved status of the structures. With the application of the BARC materials, it could be possible to generate smaller uniform patterns, enhancing the pattern size limitations of LIL. These uniform patterns could be advantages for various applications, such as fabrication of a stamp mold for nano-imprinting lithography.

Acknowledgments

This research was supported by Basic Science Research Program of the National Research Foundation of Korea (NRF) funded by the Ministry of Education, Science and Technology (No. 2009-0083126), partially supported by World Class University (WCU, R32-2008-000-10082-0), and Samsung Advanced Institute of Technology.

References

[1] A. Rodriguez, M. Echeverria, M. Ellman, N. Perez, Y.K. Verevkin, C.S. Peng, T. Berthou, Z. Wang, I. Ayerdi, J. Savall, S.M. Olaizola, Microelectron. Eng. 85 (2009) 937.
[2] M. Ellman, A. Rodriguez, N. Perez, M. Echeverria, Y.K. Verevkin, C.S. Peng, T. Berthou, Z. Wang, S.M. Olaizola, I. Ayerdi, Appl. Surf. Sci. 255 (2009) 5537.
[3] P. Zuppella, D. Luciani, P. Tucceri, P. De Marco, A. Gaudieri, J. Kaiser, L. Ottaviano, S. Santucci, A. Reale, Nanotechnology 20 (2009) 115303.
[4] C. Tan, C.S. Peng, J. Pakarinen, M. Pessa, V.N. Petryakov, Y.K. Verevkin, J. Zhang, Z. Wang, S.M. Olaizola, T. Berthou, S. Tisserand, Nanotechnology 20 (2009) 125303.
[5] F. Ma, M.H. Hong, L.S. Tan, Appl. Phys. Mater. Sci. Proc. 93 (2008) 907.
[6] R. Murillo, H.A. van Wolferen, L. Abelmann, J.C. Lodder, Microelectron. Eng. 78/79 (2005) 260.
[7] S.–.H. Hwang, K.–.K. Lee, J.–.C. Jung, Polymer 41 (2000) 6691.
[8] S. Takei, T. Shinjo, Y. Sakaida, Jpn. J. Appl. Phys. 46 (2007) 7279.
[9] Wen-Bing Kang, Hatsuyuki Tanaka, Ken Kimura, Munirathna Padmanaban, Satoru Funato, Yoshiaki Kinoshita, Takanori Kudo, Yuko Nozaki, Georg Pawlowski, J. Photopolymer Sci. Technol. 10 (1997) 471.
[10] W. Hinsberg, F.A. Houle, J. Hoffnagle, M. Sanchez, G. Wallraff, M. Morrison, S. Frank, J. Vac. Sci. Technol. B. 16 (1998) 3689.
[11] Q. Xie, M.H. Hong, H.L. Tan, G.X. Chen, L.P. Shi, T.C. Chong, J. Alloy. Comp. 449 (2008) 261.